Title

Light disrupts social memory via a retina-to-supraoptic nucleus circuit.

Permalink

https://escholarship.org/uc/item/6gc80631

Journal

EMBO Reports, 24(10)

Authors

Huang, Yu-Fan

Liao, Po-Yu

Yu, Jo-Hsien

et al.

Publication Date

2023-10-09

DOI

10.15252/embr.202356839

Peer reviewed

Light disrupts social memory via a retina-to-supraoptic nucleus circuit

Yu-Fan Huang[†] iD, Po-Yu Liao[†] iD, Jo-Hsien Yu iD & Shih-Kuo Chen (Alen)[*] iD

Abstract

The formation of social memory between individuals of the opposite sex is crucial for expanding mating options or establishing monogamous pair bonding. A specialized neuronal circuit that regulates social memory could enhance an individual's mating opportunities and provide a parallel pathway for computing social behaviors. While the influence of light exposure on various forms of memory, such as fear and object memory, has been studied, its modulation of social recognition memory remains unclear. Here, we demonstrate that acute exposure to light impairs social recognition memory (SRM) in mice. Unlike sound and touch stimuli, light inhibits oxytocin neurons in the supraoptic nucleus (SON) via M1 SON-projecting intrinsically photosensitive retinal ganglion cells (ipRGCs) and GABAergic neurons in the perinuclear zone of the SON (pSON). We further show that optogenetic activation of SON oxytocin neurons using channelrhodopsin is sufficient to enhance SRM performance, even under light conditions. Our findings unveil a dedicated neuronal circuit through which luminance affects SRM, utilizing a non-image-forming visual pathway, distinct from the canonical modulatory role of the oxytocin system.

Introduction

Oxytocin signaling plays a critical role in regulating various social and sexual behaviors, as well as recognition memory performance (Ferguson *et al*, 2000; Ross & Young, 2009; Lukas *et al*, 2011; Nakajima *et al*, 2014; Oettl *et al*, 2016). Reduction of oxytocin neurons number has been shown to be associated with social behavior disorder. Oxytocin, which is involved in pair bonding and parental behaviors, is prominently expressed in the supraoptic nucleus (SON) and paraventricular nucleus (PVN) of the hypothalamus (Armstrong, 2015; Liao *et al*, 2020). Through their central projections (Liao *et al*, 2020) and somatodendritic release (Ludwig, 1998), oxytocin neurons in these regions modulate neural activity and exert regulatory effects on memory formation and social interaction in various brain regions such as the hippocampus, central amygdala, medial amygdala, periaqueductal gray (PAG), and nucleus accumbens (NAc) (Eliava *et al*, 2016; Xiao *et al*, 2017; Liao *et al*, 2020). Understanding the upstream circuitry that modulates oxytocin neurons is important for unraveling the mechanisms underlying social behavior regulation. Recent studies have demonstrated that sensory input, including physical contact (Resendez *et al*, 2020; Tang *et al*, 2020; Yu *et al*, 2022) and auditory cues such as pup's calling during parenting (Carcea *et al*, 2021), can activate oxytocin neurons in the PVN. However, the direct modulation of oxytocin neuron activity in the PVN or SON by visual stimuli or other sensory systems remains unclear.

In addition to its role in image-forming functions, the visual system of animals also conveys light information that can influence various physiological processes and behaviors. Recent studies have highlighted the acute effects of light on physiological functions and cognitive processes. For example, light exposure has been found to impact sleep (Lupi *et al*, 2008; Chellappa *et al*, 2013; Zhang *et al*, 2021), alertness/arousal (Badia *et al*, 1991; Cajochen *et al*, 2000), anxiety (Valle, 1970; Hughes *et al*, 2014), mood (LeGates *et al*, 2012), and cognitive functions such as object and odor recognition memory (Tam *et al*, 2016; Hasan *et al*, 2021). However, a potential neuronal circuit within the visual system that could play a role in the regulation of social/sexual recognition memory remains elusive. Intrinsically photosensitive retinal ganglion cells (ipRGCs) constitute the majority of retinal innervation to various brain regions involved in non-image-forming functions. These regions include the suprachiasmatic nucleus (SCN), olivary pretectal nucleus (OPN), peri-lateral habenula (pLH), intergeniculate leaflet (IGL), and supraoptic nucleus (SON) (Hattar *et al*, 2006). Through the expression of the photopigment melanopsin, ipRGCs can directly detect light and mediate the acute effects of light on physiological functions such as arousal (Milosavljevic *et al*, 2016), body temperature, sleep (Rupp *et al*, 2019), mood (Fernandez *et al*, 2018), pupillary light reflex (Chen *et al*, 2011), and circadian photoentrainment (Hatori *et al*, 2008; Ecker *et al*, 2010). Recent studies showed that ipRGC could regulate neuronal activity in the SON such as oxytocin neurons during development and AVP neurons in adults (Hu

Department of Life Science, National Taiwan University, Taipei, Taiwan
*Corresponding author. Tel: +886 2 3366 1571; E-mail: alenskchen@ntu.edu.tw
†These authors equally contributed to this work

et al, 2022; Berry *et al*, 2023; Meng *et al*, 2023). However, the role of this circuitry in the regulation of social and sexual behavior remains unclear.

Here, we provide evidence for a visual circuit connecting the retina and the supraoptic nucleus (SON) that plays a role in modulating social recognition memory (SRM). We found that light exposure activates GABAergic interneurons located in the perinuclear zone of the SON (pSON) and inhibits oxytocin neurons in the SON, and eventually reduces SRM. By genetically eliminating ipRGCs or silencing GABAergic interneurons in the pSON region, we were able to block the light-induced reduction in SRM. These findings highlight the existence of a direct sensory circuit that transmits visual signals to modulate the oxytocin system in the brain and regulate the formation of social memory.

Results

Light negatively influences social recognition memory of mice

To test the influence of light on social recognition memory in mice, we conducted a two-trial social recognition test under dim light conditions (5 lux) using a single stimulus female. Prior to the trials, wild-type male mice were exposed to either an hour of bright light treatment (800 lux) or total darkness, referred to as the L and D groups, respectively (Fig 1A). Our findings revealed that the recognition index of the L group was significantly lower than that of the D group, indicating a negative impact of light treatment on social recognition memory (Figs 1B and C, and EV1A–C). Additionally, further investigation into the impact of light intensity revealed a dose-dependent relationship between light intensity and social recognition memory performance. Higher light intensities resulted in more pronounced impairments in social memory (Fig EV1D and F). Interestingly, the strongest light we used here (800 lx) was still not sufficient to produce statistical difference for male-to-male social memory (Fig EV1G–I) even under the same condition as male-to-female experiment, potentially due to low interaction time during the first trial. To further test the same light effect on other types of memory, we performed the novel object recognition test, which showed no significant difference between the L and D groups (Fig EV2A–E). Next, we conducted three-chamber sociability and social novelty tests for the L and D groups to investigate whether light inadvertently affected the recognition index by inhibiting sociability during the first trial (Fig EV2F). The results revealed that an hour of light treatment did not significantly impact sociability or social novelty index (Fig EV2G and H). Furthermore, the duration of investigation during the first trial was comparable between the L and D groups (Fig 1C, left panel), indicating that impaired SRM in the L group was not a result of significantly reduced social interaction during the initial trial. Together, we report a significant social memory reduction by light in a male-to-female condition. However, our tests are underpowered to find significant reductions in social memory tests between male-to-male subjects, object memory tests, and sociability tests with matching light exposure procedures and comparable sample sizes. Therefore, these results suggest that light has a profound impact on social memory.

To further test whether the disrupted social memory observed in the L group is attributed to sleep deprivation during the inter-trial interval, and hence having worse memory consolidation than the D group, we recorded the locomotor activity of mice in their home cage during the inter-trial interval (Fig EV3A). Total locomotor activity, measured by beam crossing and traveling distance, was assessed. Contrary to the expectation, the L group had lower locomotor activity and longer durations of immobility, which challenges the notion that the negative effect of light treatment on social recognition memory is caused by sleep disturbances (Fig EV3B–D). Subsequently, we examined whether shifting the 1-h light treatment to the inter-trial interval would affect SRM by impairing memory retrieval (Fig 1D). If light exposure influenced SRM through memory retrieval rather than memory formation, we would expect a lower recognition index in the inter-trial light exposure group compared to the D group. However, our data demonstrated similar recognition indices between the inter-trial L and D groups (Fig 1E and F), arguing against that light exposure may affect SRM retrieval. Taken together, our findings indicate that bright light exposure can modulate SRM, potentially by impairing the memory formation stage.

In order to examine the influence of circadian clock on light-mediated effects on social recognition memory, we conducted the experiment at CT 6, corresponding to midday (Fig EV3E). The animals were exposed to the same bright light treatment and total darkness, respectively. Surprisingly, the recognition index of the L and D groups at CT 6 was comparable (Fig EV3F). Moreover, the investigation duration of both groups at CT 6 was shorter than those at CT 12 (Fig EV3F and G). These results suggest that the regulation of social investigation and SRM is circadian clock gated, with light having minimal effect during midday. Hereafter, we perform following experiments at CT 12.

Light inhibits SON oxytocin neurons to reduce SRM

Oxytocin is a neurohormone involved in social interaction, pair bonding, and social memory formation. To confirm the involvement of oxytocin in SRM under darkness, we administered an intracerebroventricular injection of the oxytocin receptor antagonist (OTA) through an implanted cannula 30 min prior to the test (Fig 2A and B). The recognition index of OTA-injected mice was significantly lower than that of the PBS-injected control (Fig 2C and D), providing evidence for the role of oxytocin signaling in SRM. Within the hypothalamus, two main regions containing oxytocin neurons are the PVN and SON. Anatomically, both the PVN and SON receive inputs from ipRGCs through the SCN and pSON, respectively. Similar to previous report (Hu *et al*, 2022), we found that light could increase the baseline number of c-fos-positive neurons in the SON without social interaction. To explore the potential modulation of oxytocin neural activity by light in the PVN and SON for SRM, we collected brain tissue from mice 1 h after social interaction and conducted c-fos immunostaining in the light exposure and dark control groups (Fig 2E). Interestingly, we observed a significant reduction in the number of c-fos-positive SON^{OT} neurons in the L group compared to the D group (Fig 2F and H). Conversely, the small reduction in the number of c-fos-positive PVN^{OT} neurons between the L and D groups from the same set of mouse brains does not show statistical difference (Fig 2G and H). Therefore, our results suggest that light can suppress the activity of SON^{OT} neurons and we will focus our study on the regulation of SON^{OT} neurons.
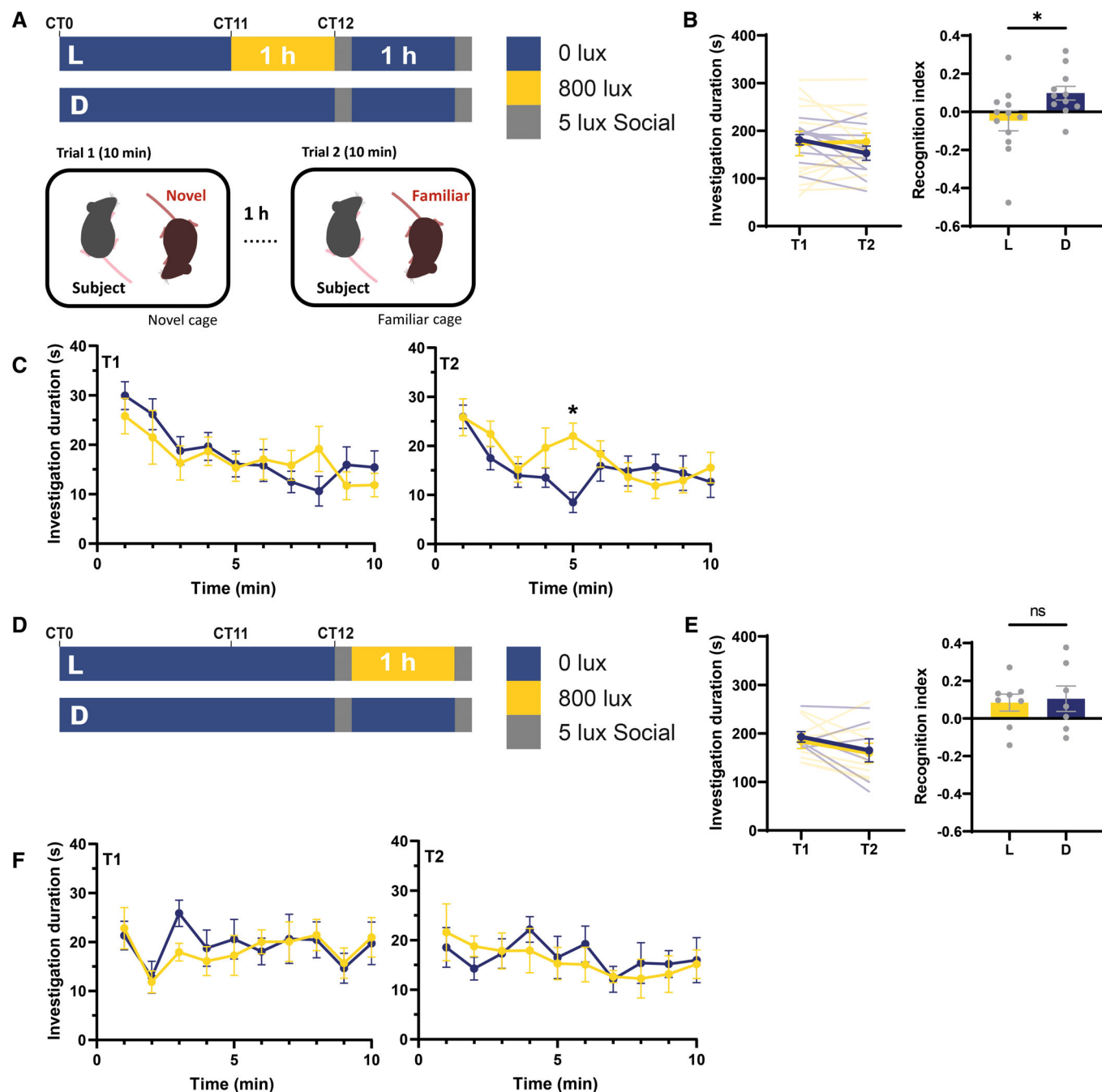
Figure 1. Social recognition memory (SRM) is impaired following pre-social light exposure.

A Schematic representation of pre-social light exposure and the two-trial social recognition test.

B Comparison of investigation duration and recognition index between the light (L, $n = 12$ animals) and dark control (D, $n = 11$ animals) groups. A significant reduction in the recognition index is observed in the L group compared to the D group (* $P = 0.0156$, Mann–Whitney test), while no significant difference is observed in investigation duration during the first trial. Data are shown as mean $\pm$ SEM.

C Minute-wise investigation duration of the L ($n = 12$ animals) and D ($n = 11$ animals) groups. The L group shows a significant increase in investigation time during the second trial (*$P = 0.0106$, Sidak's multiple-comparison test). Data are shown as mean $\pm$ SEM for each minute.

D Schematic representation of inter-trial light exposure and the social recognition test.

E No statistically significant difference is observed in the investigation duration and recognition index between the L ($n = 8$ animals) and D ($n = 7$ animals) groups ($P = 0.9551$, Mann–Whitney test). Data are shown as mean $\pm$ SEM.

F Minute-wise investigation duration of the intertrial L ($n = 8$ animals) and D ($n = 7$ animals) groups. Data are shown as mean $\pm$ SEM for each minute.

Source data are available online for this figure.
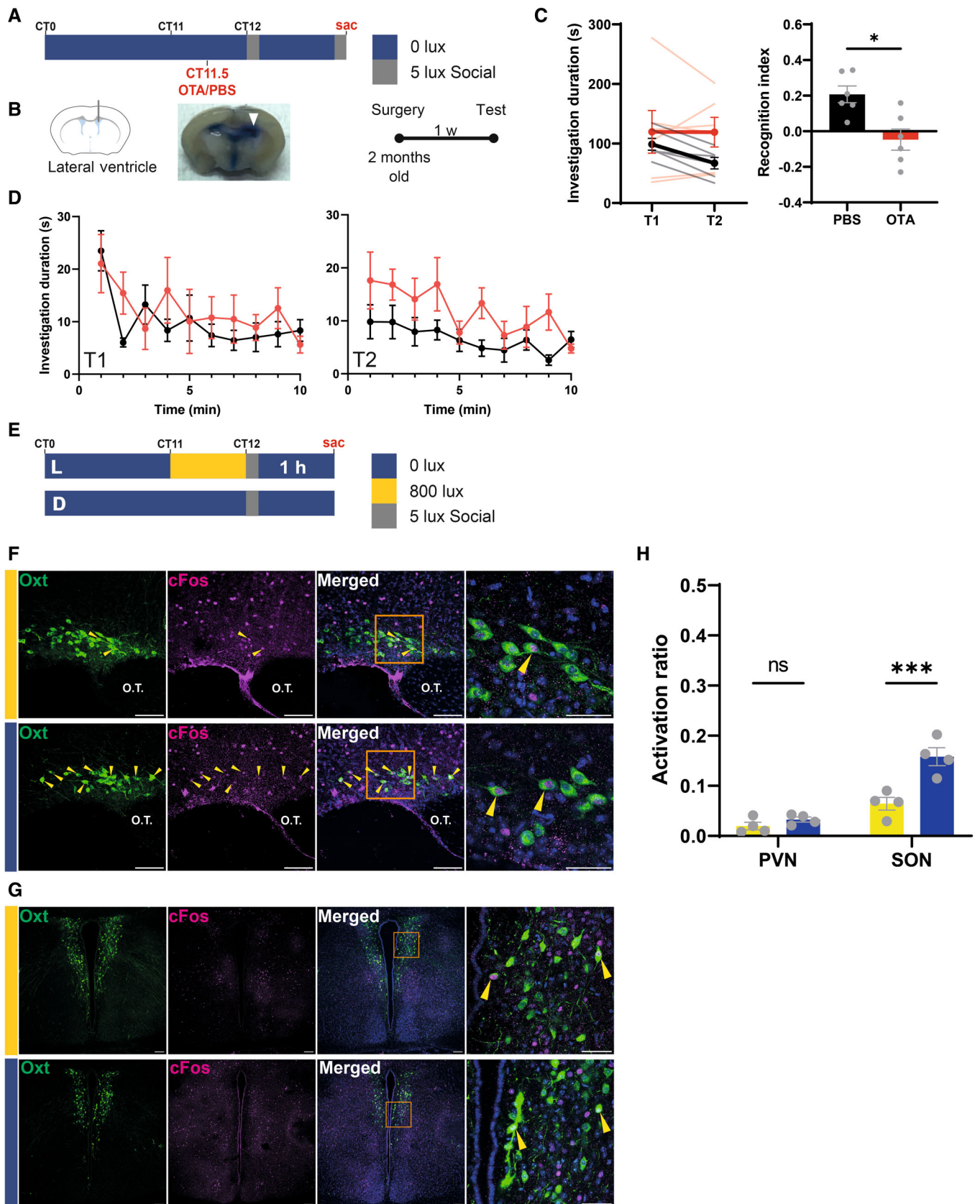
Figure 2.

Figure 2. Supraoptic oxytocin neurons are inhibited by environmental luminance.

A   Schematic representation of the social recognition test for the PBS control and OTA-treated groups.

B   Representative photograph showing a brain slice with cannula implantation into the lateral ventricle and dye verification of the implantation site. Arrowhead indicates the cannula implantation site.

C   OTA treatment ($n = 6$ animals) significantly reduces the recognition index in mice compared to the PBS injection control ($n = 6$ animals) mice (*$P = 0.0260$, Mann–Whitney test). Data are shown as mean $\pm$ SEM.

D   Minute-wise investigation duration of the OTA- ($n = 6$ animals) and PBS-treated ($n = 6$ animals) groups. Data are shown as mean $\pm$ SEM for each minute.

E   Schematic representation of the c-fos-staining experiment.

F, G   Representative confocal images of c-fos staining showing oxytocin neurons in the supraoptic nucleus (SON) (E) and paraventricular nucleus (PVN) (F) in the L and D groups. Yellow arrows indicate oxytocin neurons co-labeled with c-fos. High-magnification images are 10 μm Z-stack (63X, NA = 1.4, pinhole = 1.26 AU), while low-magnification images are 30 μm Z-stack (20X, NA = 0.7, pinhole = 1.26 AU). Scale bar = 100 μm for low-magnification images and 50 μm for high-magnification images.

H   There is a significant reduction in the c-fos-positive ratio of SON oxytocin neurons (***$P = 0.0002$, two-way ANOVA) but not PVN oxytocin neurons ($P = 0.7041$, two-way ANOVA) in the L group ($n = 4$ animals) compared to the D group ($n = 4$ animals). Left and right hemisphere c-fos-positive ratios were averaged first for each animal. Data are shown as mean $\pm$ SEM.

Source data are available online for this figure.

To further confirm light responsiveness of SON^{OT} neurons *in vivo*, we performed calcium imaging using fiber photometry. We injected AAV9/flox-GCaMP6s into the SON region and implanted an optic fiber above the SON in Oxt$^{Cre/+}$ mice (Fig 3A and B). Consistent with our expectations, the GCaMP signal from SON^{OT} neurons in Oxt$^{Cre/+}$ mice was suppressed during exposure to bright light (800 lux) compared to the baseline. The GCaMP signal during the 30 s light exposure period was lower than the baseline period (Fig 3C, black trace). To access the role of ipRGCs in suppressing SON^{OT} neurons, we performed fiber photometry in Oxt$^{Cre/+}$; Opn4$^{DTA/DTA}$ mice, where M1 ipRGCs were primarily eliminated (Chew *et al*, 2017). In contrast to Oxt$^{Cre/+}$ mice, the GCaMP signal remained unchanged during the light exposure period in Opn4$^{DTA/DTA}$ mice (Fig 3C, red trace). Moreover, the difference in mean GCaMP signal between the baseline and light exposure periods was significantly larger in control mice compared to Opn4$^{DTA/DTA}$ mice, where it was close to zero (Fig 3D). These results collectively support the essential role of ipRGCs in transmitting light information to acutely suppress the activity of SON^{OT} neurons.

The observation suggests a potential mechanism by which light-induced suppression of SON^{OT} neuronal activity prior to social encounters may contribute to the subsequent impairment of SRM. To assess whether the activation of SON^{OT} neurons can rescue the light-induced impairment of SRM, we implanted an optic fiber above the SON in Oxt$^{Cre/+}$; ROSA$^{ChR2-eYFP/+}$(Ai32) mice to manipulate the activity of SON^{OT} neurons (Fig 3E and F). Male mice were subjected

to 1 h of light exposure prior to the social recognition test, following a similar experimental setup as before. However, during the second half of the light exposure period, SON^{OT} neurons were exogenously activated using a 470 nm LED (5 Hz, 10 ms per pulse), while a separate experiment day included a negative control with opto-stimulation using a 595 nm LED (5 Hz, 10 ms per pulse) before the social recognition test. The recognition index for the 470 nm opto-stimulation group was significantly higher than that of the 595 nm control group (Fig 3G and H). These results indicate that the activation of SON^{OT} neurons could alleviate light-induced SRM reduction by potentially modulating the memory formation process.

Brn3b$^+$ M1 ipRGCs transmit environmental light information to the SON

Recent evidence suggests that distinct subtypes of ipRGCs can project to different brain regions, modulating various non-image-forming functions. Specifically, Brn3b-negative M1 ipRGCs project to the suprachiasmatic nucleus (SCN), while Brn3b-positive M1 and non-M1 ipRGCs project to other brain regions. To investigate the involvement of ipRGCs and their sub-populations in the light-induced suppression of SON^{OT} neurons, we conducted c-fos staining of SON^{OT} neurons using the same experimental conditions as previously described, but in Opn4$^{DTA/DTA}$ mice with genetically ablated M1 ipRGCs. Interestingly, we found that there was no significant difference statistically in the number of c-fos-positive SON^{OT} neurons

Figure 3. Optogenetic activation of SON^{OT} neurons during light treatment rescues light-impaired social recognition memory (SRM).

A, B   Schematics of fiber photometry recording and representative image of the implantation site. Scale bar = 100 μm.

C   Average delta-F/F signal trace from SON oxytocin neurons with 10 s of dim light (5 lux) followed by 30 s of bright light (800 lux) in OPN4$^{DTA/DTA}$; Oxt$^{Cre/+}$ mice (red line, $n = 4$ animals) and OPN4$^{+/+}$; Oxt$^{Cre/+}$ mice (black line, $n = 5$ animals). The color shade indicates standard deviation.

D   Mean change of delta-F/F 2oAC(C). There is a significant reduction in GCaMP signal in control mice after light exposure (*$P = 0.0159$, Mann–Whitney test). Data are shown as mean $\pm$ 2oACM.

E   Schematics illustrating the optogenetic activation of SON^{OT} neurons during pre-social light treatment.

F   Schematics illustrating the optogenetic activation of SON^{OT} neurons during inter-trial light treatment and the representative image of the implantation site. Scale bar = 100 μm.

G   The investigation duration and recognition index of the 595 nm control and the 470 nm activation groups ($n = 8$ animals). There is a significant increase in the recognition index in the optogenetic activation group compared to the control (**$P = 0.0078$, Wilcoxon matched-pairs signed-rank test). Data are shown as mean $\pm$ SEM.

H   Minute-wise investigation duration of the 595 nm control (black, $n = 8$ animals) and 470 nm activation (red, $n = 8$ animals) groups. Data are shown as mean $\pm$ SEM for each minute.

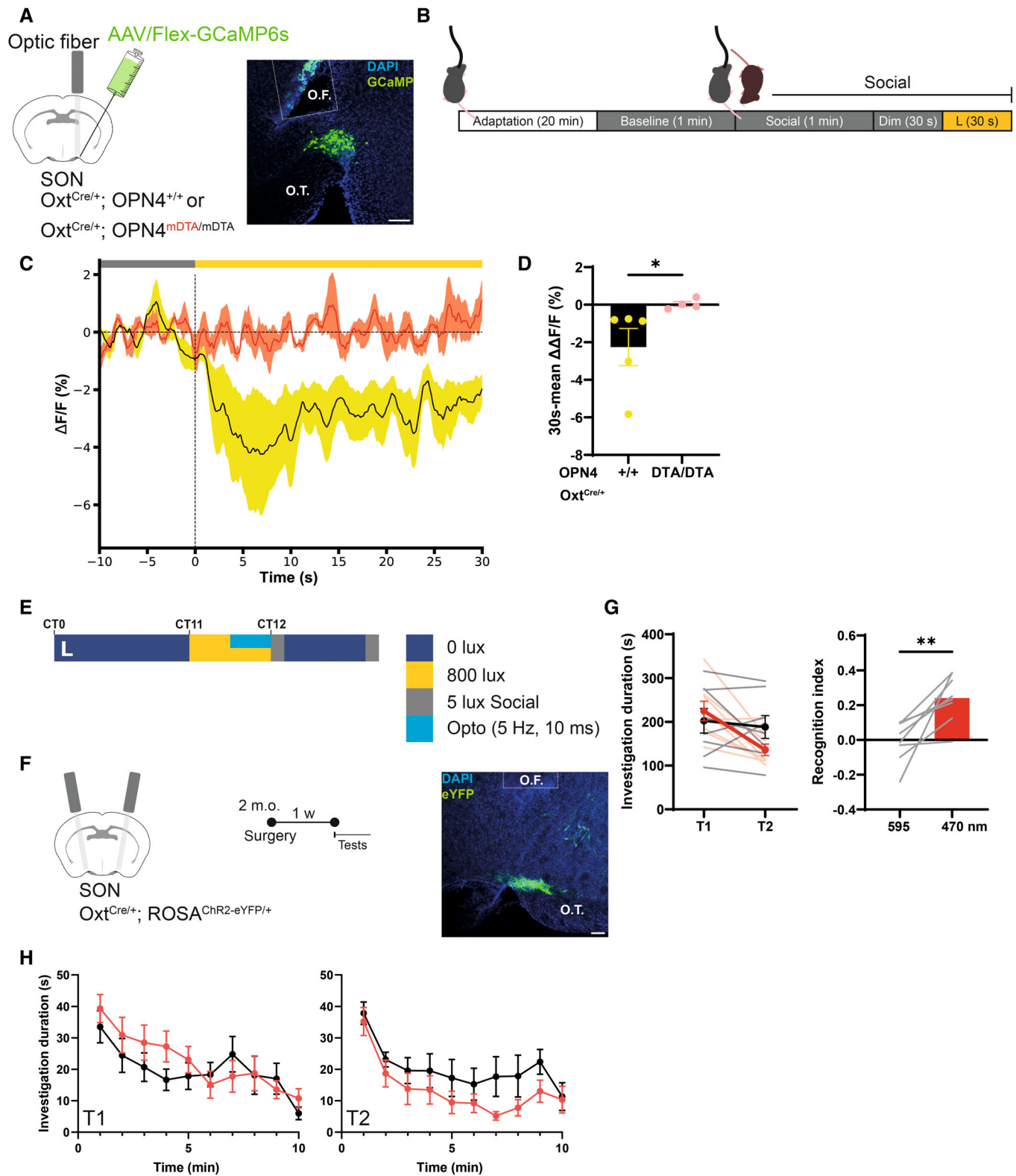Source data are available online for this figure.

Figure 3.

between the L and D groups in Opn4[DTA/DTA] mice (Fig EV4A–C). To further confirm which population of ipRGCs can modulate SON[OT] neurons, we performed c-fos staining in Opn4[Cre/+]; Brn3b[zDTA/+]

mice. In this mouse line, the ipRGC to SCN circuit and circadian photoentrainment remained functional, while the ipRGC to other brain areas such as the peri-supraoptic nucleus (pSON) was

eliminated. Similar to Opn4$^{DTA/DTA}$ mice, there was no significant difference statistically between the ratio of c-fos-positive SON^{OT} neurons from the L and D groups in Opn4$^{Cre/+}$; Brn3b$^{zDTA/+}$ mice (Fig EV4D–F). Together, the power of our tests can detect the significant light effect on the control mice but not enough to distinguish the difference between light and dark groups from two distinct ipRGC-eliminating mouse lines with similar sample sizes and experimental procedures. Collectively, these findings suggest that Brn3b-positive M1 ipRGCs, which project to many brain regions including the pSON, are essential for light-dependent inhibition of SON^{OT} neurons.

SON-projecting ipRGCs mediate modulation of social recognition by light

To investigate the requirement of melanopsin signaling and Brn3b-positive M1 ipRGCs in the light-induced modulation of SRM behaviorally, we conducted experiments using Opn4$^{Cre/+}$ control mice, Opn4$^{DTA/DTA}$ mice with genetically ablated M1 ipRGCs, and Opn4$^{Cre/+}$; Brn3b$^{zDTA/+}$ mice (Fig 4A). In control mice, the recognition index of the L group was significantly lower than the D group, consistent with the findings in wild-type (WT) mice (Fig 1B and 4B, and EV5A). However, in both Opn4$^{DTA/DTA}$ and Opn4$^{Cre/+}$; Brn3b$^{zDTA/+}$ animals, there was no significant difference statistically between the recognition indices from the L and D groups (Figs 4C and D, and EV5B and C). These data indicate that the power of our current tests cannot detect the reduction in the SRM by light in Opn4$^{DTA/DTA}$ and Opn4$^{Cre/+}$; Brn3b$^{zDTA/+}$ mice. Together, our results suggest that Brn3b-positive M1 ipRGCs, but not SCN-projecting M1 ipRGCs, are the primary conduit for light-dependent SRM reduction.

Remarkably, in melanopsin knockout (MKO) animals, we observed no significant difference in the recognition index between the L and D groups (Figs 4E and EV5D). Moreover, in the OPN4$^{Cre/+}$ control experiment, both the L and D groups showed a higher recognition index compared to OPN4$^{+/+}$ animals (Figs 1B and 4B). This observation suggests that the level of melanopsin expression and the function of melanopsin photodetection may play a crucial role in the sustained inhibition of SON^{OT} neurons and the subsequent light-induced reduction in SRM. To further confirm the capability of the signal from SON-targeting ipRGCs in modulating SRM *in vivo*, we utilized Opn4$^{Cre-ERT2/+}$; ROSA$^{ChR2-eYFP/+}$(Ai32) mice to

selectively express channelrhodopsin in ipRGCs and activated their terminals in the pSON using 470 nm LED light stimulation (10 Hz, 10 ms) delivered through an optic fiber implanted above the SON (Fig 4F and G). The recognition index in the 470-nm-stimulated trials was significantly lower than in the control 595 nm opto-stimulation trials (Fig 4H and I), indicating that the activation of SON-targeting ipRGCs alone is sufficient to reduce SRM. Taken together, our findings suggest that pSON-projecting ipRGCs are the primary conduit to modulate SRM by inhibiting SON^{OT} neurons.

ipRGCs synapse on GABAergic neurons in the perinuclear zone of the SON

According to previous studies (Theodosis *et al*, 1986; Roland & Sawchenko, 1993; Brussaard *et al*, 1997; Engelmann *et al*, 2004), it is suggested that GABA release from GABAergic interneurons within the SON may contribute to the inhibition of SON^{OT} neurons. Next, we investigate whether the indirect inhibition of SON^{OT} neurons by ipRGCs occurs through GABAergic neurons in the pSON. To explore the connectivity between ipRGCs and the SON/pSON region, we employed triple labeling using GAD67$^{eGFP/+}$ to identify GABAergic neurons, CTB-Alexa 568 injection in the eye to label RGC terminals in the pSON, and immunostaining of synaptophysin to visualize the presynaptic site (Fig 5A). Our observations revealed that ipRGC axon terminals were predominantly localized in the peri-SON region and formed numerous putative synaptic contacts on the soma of GABAergic neurons (Fig 5B–F). These findings suggest that ipRGCs may indirectly suppress SON^{OT} neurons through their interaction with GABAergic interneurons in the peri-SON region. To investigate the activation of GABAergic neurons near the SON in response to light exposure, we conducted fiber photometry recordings using GCaMP in vGAT$^{Cre/+}$ mice injected with AAV9/flox-GCaMP7f (Fig 5G and H). We observed a significant increase in the GCaMP signal during light exposure compared to the dark baseline (Fig 5I and J), indicating that GABAergic neurons in the vicinity of the SON/pSON region are potentially responsive to light stimulation. These findings suggest that GABAergic neurons in the SON/pSON region are activated by putative synaptic contacts from the retina.

Furthermore, to confirm the modulatory role of GABAergic neurons in the pSON region on SRM, we conducted optogenetic experiments in vGAT$^{Cre/+}$; ROSA$^{ChR2-eYFP/+}$(Ai32) mice by implanting an optic fiber above the pSON region. We selectively activated

Figure 4. SON-projecting ipRGCs are required and sufficient for light-induced impairment of SRM.

A   Schematics illustrating the pre-social light exposure and two-trial social recognition test for each genotype.

B   Light exposure significantly reduces the recognition index in control Opn4$^{Cre/+}$ mice (*n* = 8 animals in both the L and D group) similar to WT mice (**P* = 0.0499, Mann–Whitney test). Data are shown as mean ± SEM.

C–E There is no significant difference in recognition index between light exposure and dark control groups in OPN4$^{DTA/DTA}$ (C, *n* = 11 animals in both the L and D groups, *P* = 0.7969), OPN4$^{Cre/+}$; Brn3b$^{z-DTA/+}$ (D, *n* = 9 animals in both the L and D groups, *P* > 0.9999), and OPN4$^{Cre/Cre}$ mice (E, L group *n* = 9 animals, D group *n* = 8 animals, *P* = 0.9551) using the Mann–Whitney test. Data are shown as mean ± SEM.

F, G Schematics illustrating the optogenetic activation of SON-projecting ipRGCs under darkness and the representative image of the implantation site. Scale bar = 100 μm.

H   During the second trial, the investigation duration of the 470 nm activation group (red) was lower than the 595 nm control (black) (*n* = 7 animals, **P* = 0.011, Sidak's multiple-comparison test). Optogenetic activation of ipRGC terminals at SON with 470 nm light significantly enhances the recognition index compared to the 595 nm control (**P* = 0.0156, Wilcoxon matched-pairs signed-rank test). Data are shown as mean ± SEM.

I   Minute-wise investigation duration of the 595 nm control (black) and 470 nm activation (red) groups (*n* = 7 animals). Data are shown as mean ± SEM for each minute.

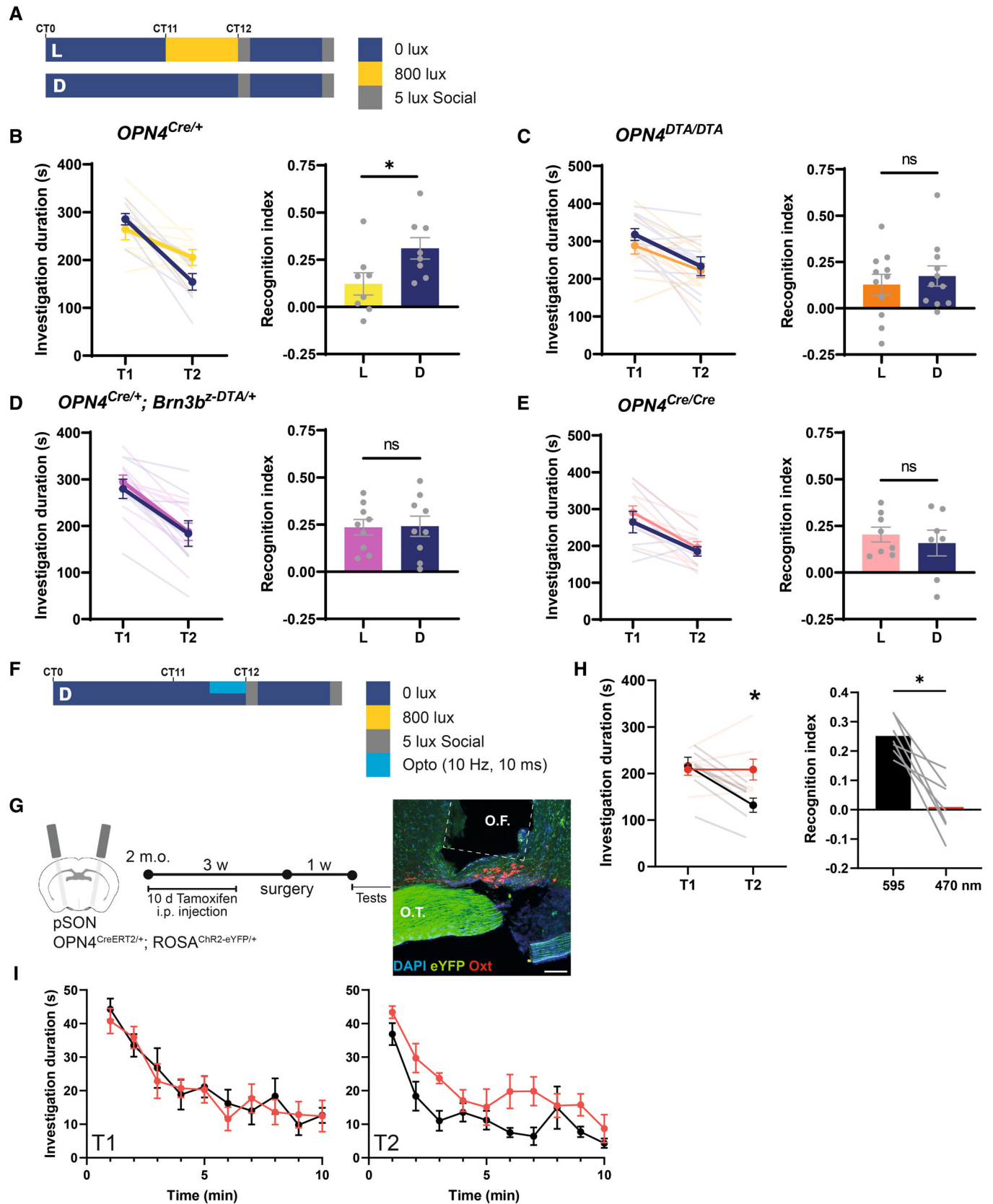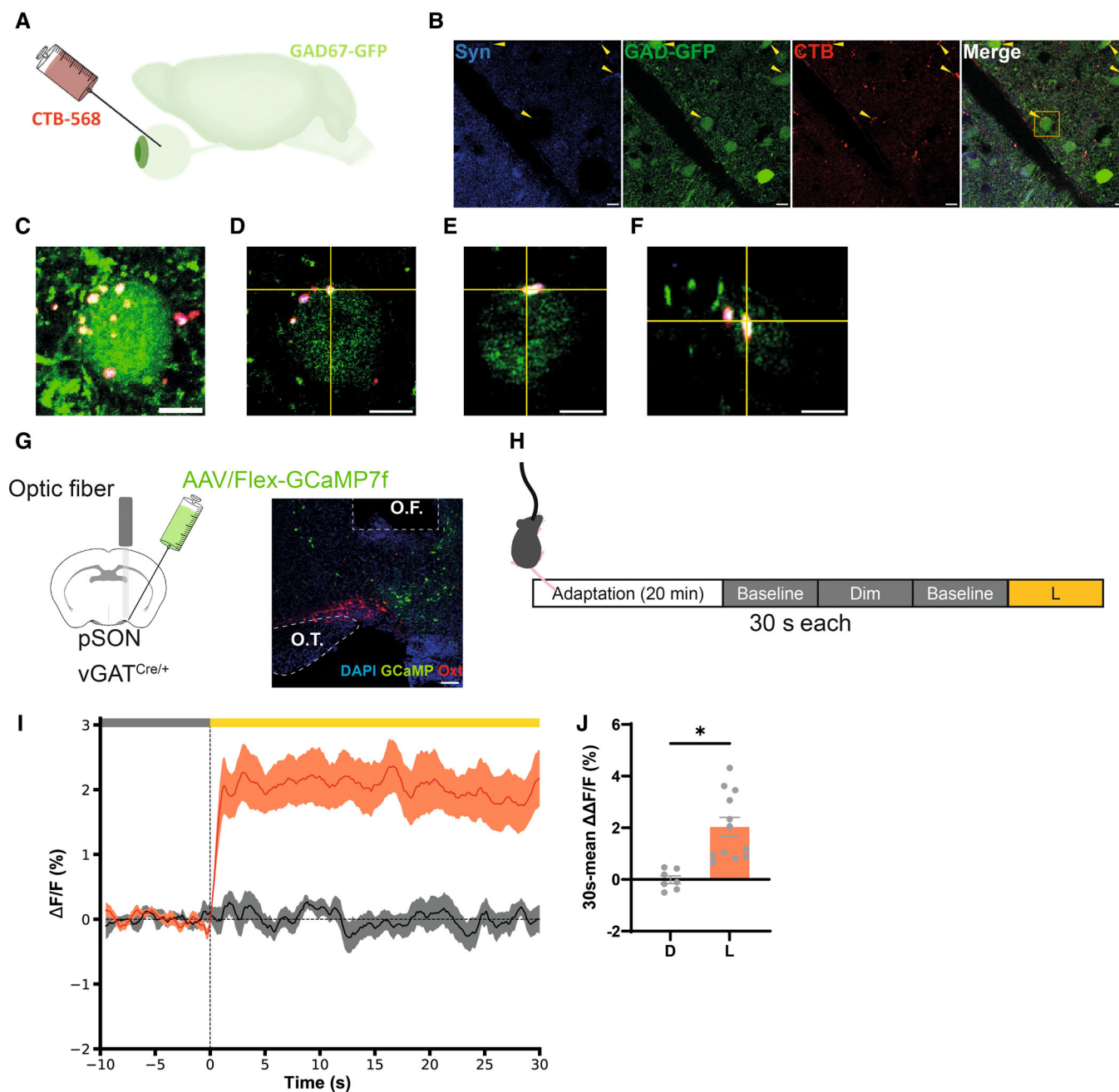Source data are available online for this figure.

Figure 4.

Figure 5. GABAergic neurons in the perinuclear zone of the SON are retino-targets and are activated by environmental light.

A   Schematics of labeling ipRGC terminals with CTB-Alexa 568 in GAD67-eGFP mice.

B   Representative confocal image of the pSON region stained with synaptophysin (blue), CTB-Alexa 568 (red), and GFP from GABAergic neurons (green). Arrowheads indicate colocalization. Scale bar = 10 μm.

C   Enlarged image of a GAD67-positive cell with colocalization of CTB-Alexa 568 and synaptophysin. White color indicates triple colocalization. Scale bar = 5 μm.

D–F Verification of colocalization at different orthogonal sections. Scale bar = 5 μm.

G, H Schematics of fiber photometry recording and the representative image of the implantation site. Scale bar = 100 μm.

I   Average delta-F/F signal trace from pSON GABAergic neurons during the transition from baseline to dim light (5 lux, black line, *n* = 7 trials) and from baseline to bright light (800 lux, red line, *n* = 12 trials) in vGAT$^{Cre/+}$ mice (*n* = 5 animals). The color shade indicates standard deviation.

J   Mean change in delta-F/F between the transitions shown in (I). Light exposure significantly increased the delta-F/F in GABAergic neurons at the pSON region (*P = 0.0156, Wilcoxon matched-pairs signed-rank test). Data are shown as mean ± SEM.

Source data are available online for this figure.

GABAergic neurons optogenetically under darkness (Fig 6A and B) and observed a significant decrease in the recognition index during the 470-nm-stimulated trials compared to the control 595-nm-stimulated trials (Fig 6C and D), providing evidence for the involvement of pSON GABAergic neurons in modulating SRM. Additionally, we selectively eliminated neurotransmitter release from pSON GABA neurons by inducing expression of tetanus toxin light chain (TeLC) using AAV9-Flex-TeLC-mCherry injected into the SON
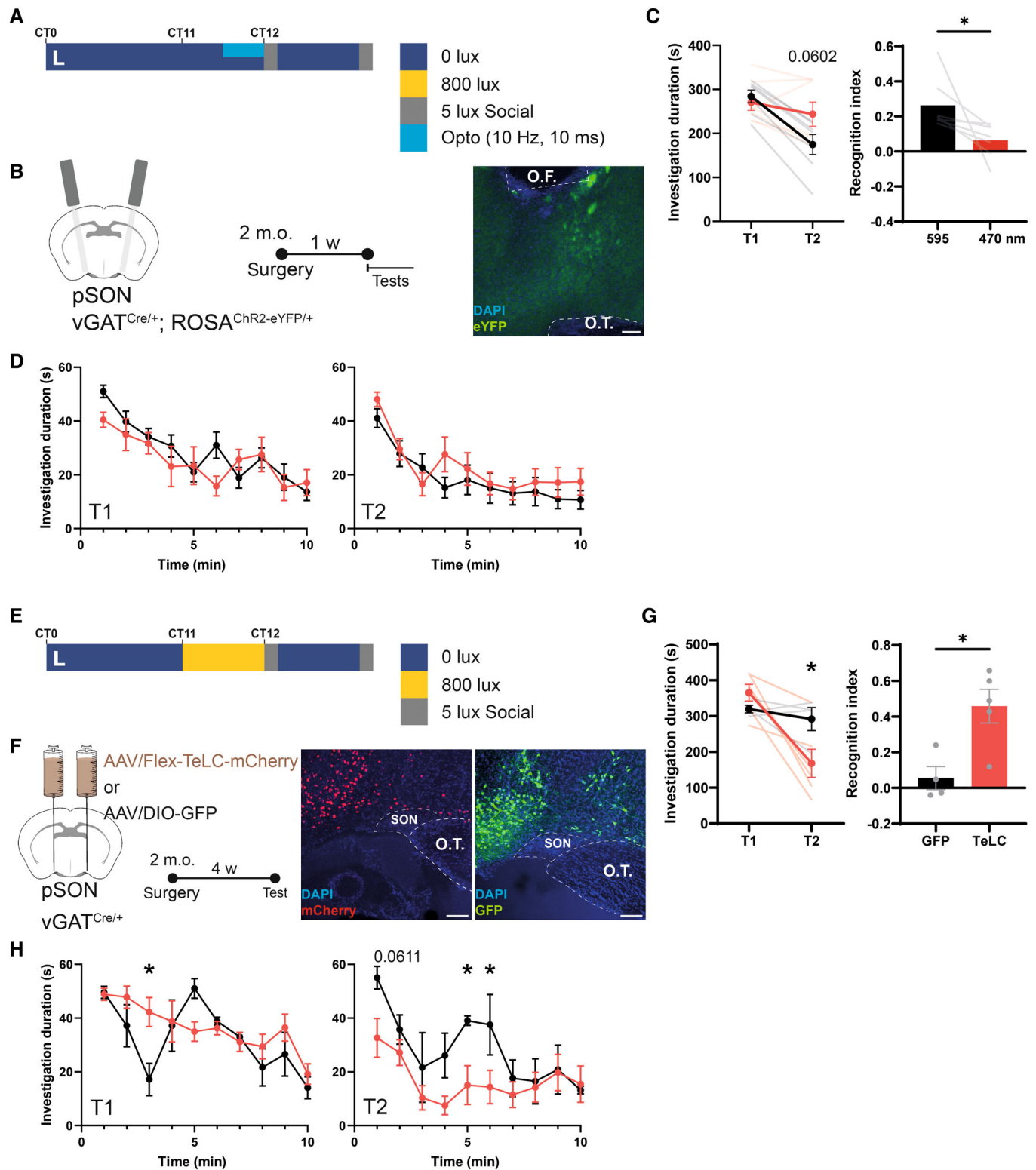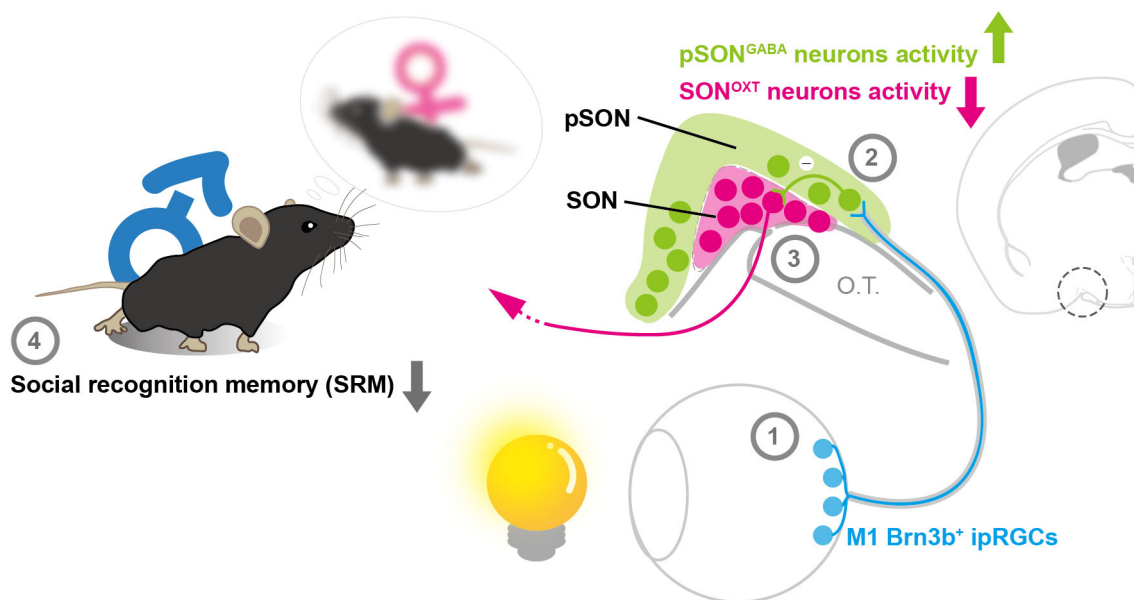

Figure 6.

Figure 7.   Graphical summary of current study.
Light reduces the activity of oxytocin neuron in the SON and SRM through ipRGCs and pSON GABAergic neurons.

of vGAT^Cre/+ mice (Fig 6E and F). This manipulation alleviated the light-induced reduction in SRM (Fig 6G and H). It is worth noting that our virus injection labeled many GABAergic neurons surrounding the SON. Whether all or only subpopulation of these GABAergic neurons are involved in light-induced SRM regulation is unclear due to technical limitations. Nevertheless, these findings suggest the activation of GABAergic neurons in the pSON vicinity as a mechanism through which light modulates SRM.

Discussion

Previous studies have established a link between light exposure and the downregulation of object and odor recognition memory in an intensity-dependent manner (Hasan *et al*, 2021). However, the impact of light on other forms of memory remains unclear. In this study, we demonstrate that optogenetic activation of ipRGC terminals or GABAergic neurons in the pSON region leads to the inhibition of SRM. This inhibition of SRM is also intensity dependent, with higher light intensities resulting in a greater reduction in SRM performance. Conversely, optogenetic activation of oxytocin neurons in the SON results in an increase in SRM. These findings suggest that ipRGCs may activate GABAergic interneurons in the pSON region, which subsequently inhibit SON^OT neurons. Therefore, our results propose a novel neuronal circuitry involving the ipRGC-pSON-SON^OT pathway, through which the light signal is conveyed to inhibit SRM (Fig 7). This circuit transmits external light information to modulate the oxytocin system in the brain, providing a direct functional input from the visual system to regulate oxytocin neurons and influence social memory via the retinohypothalamic tract (RHT) pathway.

With pre-social bright light treatment, naive wild-type male mice exhibited a significantly lower recognition index compared to dark control mice. The reduced recognition index could potentially arise from various factors, including acute inhibition of social interaction, impairment in memory formation, impairment in memory consolidation, or impairment of memory recall. However, our observations argue against the possibility of acute inhibition of social investigation. First, the *post hoc* minute-wise comparison rarely showed significant difference between L and D groups and there was no significant difference in interaction duration during the initial trial. Second, sociability and social novelty tests revealed similar indexes between the light-exposed (L) and dark control (D) groups. These findings suggest that the decrease in recognition index following light exposure is unlikely to be due to acute inhibition of social interaction.

Furthermore, it is important to note that the effects of light exposure and optogenetic activation of SON^{OT} neurons were observed predominantly before the first trial but not during the inter-trial interval. This finding indicates that light stimulation mainly influences the formation of SRM rather than impeding the recall or consolidation of SRM. This is supported by a study conducted by Ferguson *et al* (2001), where oxytocin injection in oxytocin-knockout animals before initial social exposure significantly enhanced social memory, while injection after social exposure had no effect on social memory (Ferguson *et al*, 2001). This indicates that the presence of oxytocin during the acquisition phase facilitates the processing of social cues but is not necessary for the recall of social memory. For consolidation, although direct analysis of sleep episodes was not conducted in current study, light-treated animals exhibited reduced locomotor activity and longer periods of immobility during the 1-h inter-trial period, suggesting that they did not experience sleep deprivation. Therefore, light-induced SRM reduction is unlikely due to impaired memory consolidation resulting from sleep disturbance. However, we could not rule out the possibility that light-treated mice experienced anhedonia (An *et al*, 2020).

In contrast to previous findings by Lister & Hilakivi (1988), who observed suppressed social interaction in high luminance conditions among male Swiss mice in an unfamiliar arena (Lister & Hilakivi, 1988), our study specifically focuses on measuring male-to-female investigation time. The discrepancy between our results and the previous literature could be attributed to the nature of the interactions being examined. In our experimental setup, male mice spent only around 100 s interacting with another male mouse, compared to 200–300 s with female mice. Given the relatively short interaction time during the first trial period, it is possible that our specific experimental setup could not effectively demonstrate further reduction in memory impairment with light exposure. Overall, our study provides strong evidence highlighting the significant impact of light on social recognition memory. However, further investigations utilizing alternative testing protocols are needed to determine whether light can influence social recognition memory specifically between pairs of male mice.

In addition to the experiments conducted at early night, we also investigated the impact of light exposure on SRM at midday. Surprisingly, our data revealed that SRM was close to zero in both the L and D groups during this time period. Moreover, the social interaction duration was considerably lower (around 100 s) compared to the other experimental conditions. These observations indicated a

circadian clock regulation. The observed reduction in SRM at midday may be attributed to several factors. Firstly, it is possible that the natural circadian rhythms and behavioral patterns of mice during midday contribute to decreased social investigation and memory formation. Previous studies have demonstrated that mice exhibit reduced locomotor activity and increased rest during this time, suggesting a period of reduced exploratory behavior. This decreased activity and exploration could potentially influence social interaction and memory processes, leading to the observed low recognition indexes. Secondly, it is possible that SON^{OT} neurons exhibit a circadian fluctuation of neuronal excitability and oxytocin release (Devarajan *et al*, 2005). SON^{OT} neurons may exhibit decreased activity and oxytocin release during midday, explaining that light exposure during this time did not lead to further suppression of SRM. Future investigations are required to explore the specific mechanisms underlying the reduced SRM at midday.

Previous research has established the crucial role of oxytocin in social recognition, as male mice without oxytocin exhibit impaired recognition of female mice (Ferguson *et al*, 2001). In our study, we demonstrated that ipRGCs could specifically suppress the activity of SON^{OT} neurons following light exposure, as confirmed by c-fos staining and *in vivo* calcium imaging using fiber photometry. Our findings are supported by the work of Devarajan & Rusak (2004), who reported that a nocturnal light pulse can suppress oxytocin concentration, indicative of decreased neural activity (Devarajan & Rusak, 2004). Unlike previous studies highlighting the activation of PVN^{OT} neurons through contact and sound inputs, we observed that light exposure differentially affected the activation ratio of SON^{OT} neurons but not PVN^{OT} neurons. Interestingly, the sensory inputs for regulating PVN^{OT} activity originated primarily from the somatosensory and auditory cortex, corresponding to touch and sound, respectively. Given that specific patterns of physical contact and sound, such as gentle touch and pup calling during parenting, have been shown to significantly promote oxytocin release, it is plausible that a unique sensory input and cortical computation modality are necessary to activate oxytocin neurons. In contrast, our study revealed that light, through the activation of ipRGCs and melanopsin photo-response, directly inhibited oxytocin neurons in the SON. This suggests that a simple luminance signal is sufficient to modulate the oxytocin system and its associated physiological functions. Furthermore, our findings imply that the PVN and SON may serve as distinct target sites receiving signaling inputs from different origins to regulate the oxytocin system. We speculate that under normal physiological conditions, light exposure at dawn may signal exploration rather than looking for mating opportunities. Therefore, reducing oxytocin levels and switching to food-seeking behavior may benefit individual survivability in the wild.

Previous studies have demonstrated that ipRGCs consist of distinct subpopulations, classified as M1-M6, based on their morphological and electrical characteristics. Additionally, genetic markers such as Brn3b, glycine, and GABA can further differentiate ipRGCs into functional groups. In our study, we observed that the activation ratio of SON^{OT} neurons, as indicated by c-fos staining, did not differ between the L and D groups in Opn4$^{DTA/DTA}$ and Opn4$^{Cre/+}$; Brn3b$^{zDTA/+}$ mice. Furthermore, the recognition indices were similar between the L and D groups in two different ipRGC-eliminated mice. In a previous study by Li & Schmidt (2018), the absence of ipRGC innervation in the SON was observed in Opn4$^{Cre/tau-LacZ}$;

Brn3b[z-DTA/+] mice (Li & Schmidt, 2018). Collectively, our findings suggest that Brn3b+ M1 ipRGCs serve as the primary retinal input to the SON for modulating the activity of oxytocin neurons. Without ipRGC projection, SON[OT] neural activity and SRM are no longer modulated by environmental light. Interestingly, we observed that light exposure was unable to modulate SRM in the absence of melanopsin (with ipRGCs intact), indicating the essential role of melanopsin photodetection for sustained inhibition of SON[OT] neurons. This phenomenon distinguishes it from other ipRGC-dependent functions such as circadian photoentrainment, where rod and cone signals can compensate for the absence of melanopsin. Due to the prolonged and weakly adapting nature of the melanopsin photodetection system compared to rods and cones (Berson et al, 2002), sustained activation of the ipRGC-SON circuit is likely necessary to modulate oxytocin and SRM. Collectively, our results highlight the important role of melanopsin in modulating physiological functions.

Recent studies have provided insights into the neurotransmitter release profiles of ipRGCs. While most ipRGCs release glutamate and PACAP as neurotransmitters, a subset of ipRGCs in the suprachiasmatic nucleus (SCN) has been shown to co-release GABA alongside glutamate (Sonoda et al, 2020). However, in the context of SON-innervating ipRGCs, it has been reported that these cells predominantly release glutamate (Berry et al, 2023). In our study, we discovered that ipRGCs can inhibit SON[OT] neurons following light exposure. This inhibition may occur through direct contact and GABA release or via an indirect pathway. Our data revealed numerous synaptic contacts between retinal ganglion cell (RGC) terminals and the soma of GABAergic neurons in the perinuclear zone of the SON (pSON). Previous studies have demonstrated that GABAergic input to the SON can decrease the firing rate of oxytocin neurons (Brussaard et al, 1997; Engelmann et al, 2004; Lee et al, 2015). Although our study did not completely eliminate the possibility of a small parallel pathway in which ipRGCs directly inhibit SON[OT] neurons through GABA release, we demonstrated that the activation of pSON GABAergic neurons is both necessary and sufficient to modulate SRM behaviorally. Notably, a recent study by Hu et al (2022) demonstrated that ipRGCs could activate SON[OT] neurons during the early postnatal stage (Hu et al, 2022). Although their findings presented contrasting effects of light on oxytocin content in the brain compared to our study, it is important to consider that our experiments were conducted in adult mice after sexual maturation. This raises three potential hypotheses to explain the discrepant results. First, GABAergic circuits may act as a positive stimulus for oxytocin neurons in the SON during the early postnatal period, thereby enabling light to activate SON[OT] neurons through the same pathway proposed in our study. Second, SON[OT] neurons may be divided into two groups, one group is directly activated by ipRGCs, and another group is indirectly inhibited by ipRGC through GABAergic neurons specifically during social interaction. Finally, the circuit from ipRGC to oxytocin neurons in the SON may not be a direct di-synaptic connection in adult mice. Additional brain regions downstream of ipRGC may serve as a bridge in conveying light information to SON to reduce SRM. Conducting further studies to investigate the functional or anatomical changes in the ipRGC circuitry could provide additional insights into this phenomenon.

Overall, our findings reveal a functional circuitry originating from ipRGCs to modulate the oxytocin system in the SON. In addition to touch and sound sensory inputs, luminance signals from the visual system can also modulate SRM and potentially other oxytocin-related physiological functions. Finally, the ipRGC-pSON[GABA]-SON[OT] circuitry that we propose may serve as a parallel pathway within the visual system to regulate oxytocin content in the brain. This suggests that canonical vision input can function as salient interaction stimulation during social interactions to regulate social behaviors.

Material and Methods

Animals

Adult C57BL/6J wild-type (WT) mice were purchased from the National Laboratory Animal Center (NLAC), Taipei, Taiwan. Other transgenic mice used in this study were kept and bred at the Animal Facility of the Department of Life Science at National Taiwan University, Taipei, Taiwan. All transgenic mouse lines were maintained on a C57BL/6J background. Animals were housed under 12:12 h light–dark cycle (lights on 0800-2000) at a temperature of 22°C, and had *ad libitum* access to normal chow and water unless otherwise stated. Experiments were approved by the Institutional Animal Ethics Committee of National Taiwan University, Taipei, Taiwan, and conducted in accordance with guidelines of the National Laboratory Animal Center. The RRID for Opn4[Cre] mouse is IMSR_JAX:035925, for Opn4[DTA] mouse is IMSR_JAX:035927, for Opn4[CreERT2] mouse is IMSR_JAX:035926, for Oxt[Cre] mouse is IMSR_JAX:024234, for ROSA[ChR2-eYFP]Ai32 mouse is IMSR_JAX:024109, and for GAD67[eGFP] mouse is IMSR_JAX:003718. Sample size was estimated according to prior experiments.

Two-trial social recognition tests

Two-trial social recognition tests were conducted following the established protocol. Female mice from NLAC with wild-type backgrounds were obtained and used only once, each paired with a single male subject. The male subjects were individually housed and kept in social isolation for at least 1 week prior to the experiment. To ensure consistent conditions, both the male subjects and female stimuli mice were kept in constant darkness (DD) for 1 day before the experiment. The two-trial social recognition test took place at CT 6 and CT 12.

During the test trial, the male subject was transferred to a novel cage and introduced to a female mouse for a duration of 10 min under dim light conditions (5 lux). Following the completion of the first trial, the male and female were returned to their respective home cages and kept in complete darkness (0 lux) for a period of 1 h. Subsequently, the second trial was conducted in the same cage as the first trial, using the same female stimulus. In one experimental condition, an hour of bright light treatment (800 lux) was administered prior to the social recognition test at CT 11. In another condition, the bright light treatment was given between the two trials at CT 12. In the third condition, the bright light treatment was given prior to the social recognition test at CT 5.

Throughout the test trials, the interactions within the cage were recorded using an infrared camera to capture the behavioral responses of the male subjects and the female stimuli. Recording

files were numbered without experimental conditions for blind scoring of interaction time. The recognition index was calculated as the following equation, where T1 and T2 are the total time spent on the social investigation during the first and the second trials, respectively.

$$\text{Social recognition memory index} = (T1 - T2)/(T1 + T2).$$

Three-chamber test

Three-chamber test was performed under dim light (5 lux) in a rectangular acrylic apparatus comprised of three chambers measuring 30×30 cm each, with two metal cups placed in the corner of each side chamber. Male subject mice and stimulus female mice were housed in same conditions as mice in social interaction assay. Mice habituated in the apparatus alone for 5 min and were reintroduced into the center compartment at the beginning of each 5 min phase. At CT12, a naive WT female mouse was put in the metal cup of either side compartment (Phase 1), then another stranger female mouse was placed into the other cup (Phase 2). Animals were sent back to their home cages in the darkness for 1 h, after which the first female mouse and second stranger female were introduced into the cups (Phase 3). Behaviors were recorded and analyzed with ANY-Maze (San Diego Instruments). Time spent close to the metal cups was detected and their difference was analyzed for sociability (P1) and social novelty (P2) (and social memory (P3)) for both D/L groups.

Novel object recognition test

NORT was performed in testing cage measuring 16×13 cm, following paradigm modified from Lueptow, 2017. Subject mice were housed in same conditions as mice in social interaction assay. Briefly, mice habituated in the cage for 5 min and were reintroduced before both 10 min trials. During first trial at CT12, two identical transparent plastic tubes were placed at opposite corners in the cage (Trial 1), and one of the tubes was replaced by a dark glass bottle in Trial 2. Between two trials animals were sent back to their home cage for 1 h in the darkness. Behaviors were recorded and analyzed with ANY-maze (San Diego Instruments). Time spent investigating the objects was detected and the discrimination index ($T_{novel} - T_{familiar} / T_{novel} + T_{familiar}$) was compared between D/L groups.

Inter-trial locomotor activity recording

Following the completion of the first trial of the two-trial social recognition test, the male subjects were returned to their individual home cages. Subsequently, a 1-h video recording of their behavior was conducted using an infrared camera. The recorded videos were then analyzed automatically using ANY-maze software.

The ANY-maze software was utilized to track the position of the animals throughout the recorded session. Various behavioral parameters, including the total time spent mobile and immobile, the speed of their movement, and the number of line crossings, were quantitatively analyzed using the software. These analyses provide insights into the locomotor activity and exploratory behavior of the male subjects during the post-trial period.

Stereotaxic injection

Animals were initially anesthetized with gaseous isoflurane. For the SON, the stereotaxic coordinates were -0.82 mm from bregma, ± 1.35 mm lateral from the midline, and 5.4 mm below the surface of the skull. Glass needles with a 20 μm diameter at the tip were filled with oil and connected to a Hamilton syringe (#700, 5 μl) for viral injection. A volume of 300 nl of virus was infused into the SON at a rate of 50 nl/min. The GCaMP (Addgene #104492 and Addgenev#100842) and TeLC (Addgene #159102) AAV vectors were obtained from Addgene and prepared in-house. For optic fiber implantation, the fiber was gradually lowered into the brain at a speed of approximately 0.5 mm/min using a cannula holder (RWD, 68214, China). Dental cement (Hygenic, USA) was applied to secure the optic fiber to the skull. Unilateral implantation of the optic fiber was performed using the same stereotaxic coordinates as the viral injection. For bilateral implantation (optogenetics), the fibers were tilted at a 10-degree angle toward the midline. The stereotaxic coordinates for bilateral implantation at the SON were -0.82 mm from bregma, ± 1.61 mm lateral from the midline, and 5.35 mm below the cortical surface. For pharmacological experiment, cannulas were placed into the lateral ventricle (LV) (+0.02 mm (AP); -0.84 mm (ML); -2.22 mm (DV)) and secured with denture resin (Coltene Whaledent), with two screws fastened on the skull to provide additional friction. Home-made cannulas were prepared with modified protocol from Kokare *et al* (2011). Briefly, 23-gauge stainless metal needles were grinded to make the guide cannula, while 30-gauge stainless metal needles were grinded to make the internal and dummy cannula. Central infusion of 1X PBS (1 μl) or oxytocin receptor antagonist d(CH2) 51, Tyr(Me) 2, Thr4, Orn8, and des-Gly-Nh29—vasotocin trifluoroacetate salt (OTA; 1 ng/μl, BACHEM, #1065058)—was performed at CT 11.5 under dim red light.

Eye injections

Animals were anesthetized with avertin (2,2,2-tribromoehanol; Sigma Aldrich; 20 mg/ml). Hamilton syringe (#1700, 50 μl) and needle made from glass capillaries (World Precision Instruments, #4878) were used to deliver the injection. For RGC labeling, intravitreal injections of 2 μl anterograde tracer CF®568 Cholera Toxin Subunit B (CTβ) (Biotium, #00071) were performed on GAD67-GFP mice.

Immunohistochemistry staining

Mice were deeply anesthetized with 1 ml (overdose) of Avertin (2, 2, 2-tribromoethanol; Sigma Aldrich, 20 mg/ml) and perfused intracardially with 12 ml of iced PBS, following 25 ml of 4% paraformaldehyde (PFA). Brains were collected from the perfused animals and post-fixed in the same fixative at 4°C overnight. The 80-μm-thick coronal brain sections were obtained using a vibratome (Campden Instruments, UK). For immunostaining, brain slices were incubated in blocking solution (6% goat serum in $1 \times PBST_{0.2\%}$) for 2 h at room temperature. Rabbit anti-oxytocin (Immunostar #1607001, 1:5,000), chicken anti-synaptophysin (Abcam ab130436, 1:1,000), and mouse IgG1α anti-c-fos (Abcam ab208942, 1:1,000) were diluted in blocking solution. Samples were incubated on an orbital shaker with primary antibody at 4°C overnight. Brain sections were washed and incubated in secondary antibody solution with goat anti-rabbit

(Biotium, 1:500), goat anti-mouse IgG1α, and goat anti-chicken (Invitrogen, 1:500) for 2 h at room temperature. After washing, brain slices were mounted in mounting solution (Vectashield hard set with DAPI). Images were acquired using an inverted phase contrast fluorescence microscope (Zeiss Axio Observer Z1).

Fiber photometry recording

The fiber photometry recording system was custom-built based on the schematics on Thorlabs' website (Thorlab, USA). The system consisted of two excitation sources, 405 nm and 470 nm LEDs. The LEDs were alternately turned on and off at 200 Hz in a square pulse pattern, which was driven by a PowerLab (ADInstruments, New Zealand). The illumination power of the LEDs was tuned to 0.4–0.9 mW/mm^2 for the 405 nm LED and 0.7–1.4 mW/mm^2 for the 470 nm LED at the tip of the optic fiber by LED drivers (Patel *et al*, 2020). Finally, GCaMP fluorescence was detected by a photodiode and the PowerLab at 1 kHz sampling rate. The fluorescence signal was processed by custom-written Python codes referencing the open-source toolbox GuPPy (Sherathiya *et al*, 2021). During data processing, the signals were down-sampled to 100 Hz. The 405 nm LED exciting signal was used as the isosbestic control. After both signals were low-pass filtered at 4 Hz, the isosbestic control was fitted to the data (F_{470}) using a least squares polynomial fit of degree 1, creating a fitted control ($F_{fitted\ control}$) as a result. ΔF/F was calculated by subtracting the fitted control from the data, and then dividing by the fitted channel.

$$\Delta F/F = (F_{470} - F_{fitted\ control})/F_{fitted\ control}.$$

The mice were kept in constant darkness for 1 day, then placed into recording cages and allowed to rest for 10 min while the LED excitation was turned on. Throughout this process, the environment was maintained under dim light conditions (5 lux). First, baseline was recorded for 1 min, and a stimulus female mouse was introduced to the cage to interact with the subject for a duration of 1 min. Following the interaction period, dim-to-bright light transitions were recorded. During each transition, the two mice initially interacted under dim light for 30 s, after which the entire cage was illuminated by white LED light, providing a bright light condition (800 lux), for an additional 30 s. The social interaction between the mice during the recording session was captured by an infrared camera, allowing for subsequent video analysis. For fiber photometry of pSON^{GABA} neurons, the recording session commenced with a dim-to-dim light control followed by dim-to-bright light trials, with each lighting condition lasting 30 s.

Optogenetic activation

Preparations for the social recognition test followed the description above. The male subject was tethered to the optic fiber cable at CT11 under darkness (0 lux) or bright light (800 lux) according to description. At CT11.5 to CT12, the subject was optogenetically stimulated with blue light (470 nm, 10 ms duration, 5 Hz for SON^{OT} activation, and 10 Hz for ipRGC and SON^{GABA}) or amber light (595 nm) as control. The light intensity was adjusted to 4 mW at the fiber tip. From CT12, the social recognition test proceeded as previously described.

Data availability

This study includes no data deposited in external repositories.

Expanded View for this article is available online.

Author contributions

Yu-Fan Huang: Conceptualization; data curation; formal analysis; validation; investigation; visualization; methodology; writing – original draft; writing – review and editing. **Po-Yu Liao:** Conceptualization; data curation; formal analysis; validation; investigation; visualization; methodology; writing – original draft; writing – review and editing. **Jo-Hsien Yu:** Data curation; formal analysis; validation; investigation; methodology; writing – review and editing. **Shih-Kuo Chen:** Conceptualization; supervision; funding acquisition; validation; investigation; writing – original draft; project administration; writing – review and editing.

Disclosure and competing interests statement

The authors declare that they have no conflict of interest.

References

An K, Zhao H, Miao Y, Xu Q, Li Y-F, Ma Y-Q, Shi Y-M, Shen J-W, Meng J-J, Yao Y-G *et al* (2020) A circadian rhythm-gated subcortical pathway for nighttime-light-induced depressive-like behaviors in mice. *Nat Neurosci* 23: 869–880

Armstrong WE (2015) Chapter 14 – Hypothalamic supraoptic and paraventricular nuclei. In *The rat nervous system*, Paxinos G (ed), 4th edn, pp 295–314. San Diego: Academic Press

Badia P, Myers B, Boecker M, Culpepper J, Harsh JR (1991) Bright light effects on body temperature, alertness, EEG and behavior. *Physiol Behav* 50: 583–588

Berry MH, Moldavan M, Garrett T, Meadows M, Cravetchi O, White E, Leffler J, von Gersdorff H, Wright KM, Allen CN (2023) A melanopsin ganglion cell subtype forms a dorsal retinal mosaic projecting to the supraoptic nucleus. *Nat Commun* 14: 1492

Berson DM, Dunn FA, Takao M (2002) Phototransduction by retinal ganglion cells that set the circadian clock. *Science* 295: 1070–1073

Brussaard AB, Kits KS, Baker RE, Willems WPA, Leyting-Vermeulen JW, Voorn P, Smit AB, Bicknell RJ, Herbison AE (1997) Plasticity in fast synaptic inhibition of adult oxytocin neurons caused by switch in GABAA receptor subunit expression. *Neuron* 19: 1103–1114

Cajochen C, Zeitzer JM, Czeisler CA, Dijk D-J (2000) Dose-response relationship for light intensity and ocular and electroencephalographic correlates of human alertness. *Behav Brain Res* 115: 75–83

Carcea I, Caraballo NL, Marlin BJ, Ooyama R, Riceberg JS, Mendoza Navarro JM, Opendak M, Diaz VE, Schuster L, Alvarado Torres MI *et al* (2021) Oxytocin neurons enable social transmission of maternal behaviour. *Nature* 596: 553–557

Chellappa SL, Steiner R, Oelhafen P, Lang D, Götz T, Krebs J, Cajochen C (2013) Acute exposure to evening blue-enriched light impacts on human sleep. *J Sleep Res* 22: 573–580

Chen SK, Badea TC, Hattar S (2011) Photoentrainment and pupillary light reflex are mediated by distinct populations of ipRGCs. *Nature* 476: 92–95

Chew KS, Renna JM, McNeill DS, Fernandez DC, Keenan WT, Thomsen MB, Ecker JL, Loevinsohn GS, VanDunk C, Vicarel DC *et al* (2017) A subset of ipRGCs regulates both maturation of the circadian clock and segregation of retinogeniculate projections in mice. *Elife* 6: e22861

Devarajan K, Rusak B (2004) Oxytocin levels in the plasma and cerebrospinal fluid of male rats: effects of circadian phase, light and stress. *Neurosci Lett* 367: 144–147

Devarajan K, Marchant EG, Rusak B (2005) Circadian and light regulation of oxytocin and parvalbumin protein levels in the ciliated ependymal layer of the third ventricle in the C57 mouse. *Neuroscience* 134: 539–547

Ecker JL, Dumitrescu ON, Wong KY, Alam NM, Chen SK, Legates T, Renna JM, Prusky GT, Berson DM, Hattar S (2010) Melanopsin-expressing retinal ganglion-cell photoreceptors: cellular diversity and role in pattern vision. *Neuron* 67: 49–60

Eliava M, Melchior M, Knobloch-Bollmann HS, Wahis J, da Silva GM, Tang Y, Ciobanu AC, Triana Del Rio R, Roth LC, Althammer F *et al* (2016) a new population of parvocellular oxytocin neurons controlling magnocellular neuron activity and inflammatory pain processing. *Neuron* 89: 1291–1304

Engelmann M, Bull PM, Brown CH, Landgraf R, Horn TFW, Singewald N, Ludwig M, Wotjak CT (2004) GABA selectively controls the secretory activity of oxytocin neurons in the rat supraoptic nucleus. *Eur J Neurosci* 19: 601–608

Ferguson JN, Young LJ, Hearn EF, Matzuk MM, Insel TR, Winslow JT (2000) Social amnesia in mice lacking the oxytocin gene. *Nat Genet* 25: 284–288

Ferguson JN, Aldag JM, Insel TR, Young LJ (2001) Oxytocin in the medial amygdala is essential for social recognition in the mouse. *J Neurosci* 21: 8278–8285

Fernandez DC, Fogerson PM, Lazzerini Ospri L, Thomsen MB, Layne RM, Severin D, Zhan J, Singer JH, Kirkwood A, Zhao H *et al* (2018) Light affects mood and learning through distinct retina-brain pathways. *Cell* 175: 71–84

Hasan S, Tam SKE, Foster RG, Vyazovskiy VV, Bannerman DM, Peirson SN (2021) Modulation of recognition memory performance by light and its relationship with cortical EEG theta and gamma activities. *Biochem Pharmacol* 191: 114404

Hatori M, Le H, Vollmers C, Keding SR, Tanaka N, Buch T, Waisman A, Schmedt C, Jegla T, Panda S (2008) Inducible ablation of melanopsin-expressing retinal ganglion cells reveals their central role in non-image forming visual responses. *PLoS One* 3: e2451

Hattar S, Kumar M, Park A, Tong P, Tung J, Yau K-W, Berson DM (2006) Central projections of melanopsin-expressing retinal ganglion cells in the mouse. *J Comp Neurol* 497: 326–349

Hu J, Shi Y, Zhang J, Huang X, Wang Q, Zhao H, Shen J, Chen Z, Song W, Zheng P *et al* (2022) Melanopsin retinal ganglion cells mediate light-promoted brain development. *Cell* 185: 3124–3137.e15

Hughes RN, Hancock NJ, Henwood GA, Rapley SA (2014) Evidence for anxiolytic effects of acute caffeine on anxiety-related behavior in male and female rats tested with and without bright light. *Behav Brain Res* 271: 7–15

Kokare DM, Shelkar GP, Borkar CD, Nakhate KT, Subhedar NK (2011) A simple and inexpensive method to fabricate a cannula system for intracranial injections in rats and mice. *J Pharmacol Toxicol Methods* 64: 246–250

Lee SW, Kim Y-B, Kim JS, Kim WB, Kim YS, Han HC, Colwell CS, Cho Y-W, In Kim Y (2015) GABAergic inhibition is weakened or converted into excitation in the oxytocin and vasopressin neurons of the lactating rat. *Mol Brain* 8: 34

LeGates TA, Altimus CM, Wang H, Lee H-K, Yang S, Zhao H, Kirkwood A, Weber ET, Hattar S (2012) Aberrant light directly impairs mood and learning through melanopsin-expressing neurons. *Nature* 491: 594–598

Li JY, Schmidt TM (2018) Divergent projection patterns of M1 ipRGC subtypes. *J Comp Neurol* 526: 2010–2018

Liao PY, Chiu YM, Yu JH, Chen S-K (2020) Mapping central projection of oxytocin neurons in unmated mice using cre and alkaline phosphatase reporter. *Front Neuroanat* 14: 559402

Lister RG, Hilakivi LA (1988) The effects of novelty, isolation, light and ethanol on the social behavior of mice. *Psychopharmacology* 96: 181–187

Ludwig M (1998) Dendritic release of vasopressin and oxytocin. *J Neuroendocrinol* 10: 881–895

Lueptow LM (2017) Novel object recognition test for the investigation of learning and memory in mice. *J Vis Exp* 55718. https://doi.org/10.3791/55718

Lukas M, Toth I, Reber SO, Slattery DA, Veenema AH, Neumann ID (2011) The neuropeptide oxytocin facilitates pro-social behavior and prevents social avoidance in rats and mice. *Neuropsychopharmacology* 36: 2159–2168

Lupi D, Oster H, Thompson S, Foster RG (2008) The acute light-induction of sleep is mediated by OPN4-based photoreception. *Nat Neurosci* 11: 1068–1073

Meng J-J, Shen J-W, Li G, Ouyang C-J, Hu J-X, Li Z-S, Zhao H, Shi Y-M, Zhang M, Liu R *et al* (2023) Light modulates glucose metabolism by a retina-hypothalamus-brown adipose tissue axis. *Cell* 186: 398–412.e317

Milosavljevic N, Cehajic-Kapetanovic J, Procyk CA, Lucas RJ (2016) Chemogenetic activation of melanopsin retinal ganglion cells induces signatures of arousal and/or anxiety in mice. *Curr Biol* 26: 2358–2363

Nakajima M, Görlich A, Heintz N (2014) Oxytocin modulates female sociosexual behavior through a specific class of prefrontal cortical interneurons. *Cell* 159: 295–305

Oettl L-L, Ravi N, Schneider M, Scheller Max F, Schneider P, Mitre M, da Silva Gouveia M, Froemke Robert C, Chao Moses V, Young WS *et al* (2016) Oxytocin enhances social recognition by modulating cortical control of early olfactory processing. *Neuron* 90: 609–621

Patel AA, McAlinden N, Mathieson K, Sakata S (2020) Simultaneous electrophysiology and fiber photometry in freely behaving mice. *Front Neurosci* 14: 148

Resendez SL, Namboodiri VMK, Otis JM, Eckman LEH, Rodriguez-Romaguera J, Ung RL, Basiri ML, Kosyk O, Rossi MA, Dichter GS *et al* (2020) Social stimuli induce activation of oxytocin neurons within the paraventricular nucleus of the hypothalamus to promote social behavior in male mice. *J Neurosci* 40: 2282–2295

Roland BL, Sawchenko PE (1993) Local origins of some GABAergic projections to the paraventricular and supraoptic nuclei of the hypothalamus in the rat. *J Comp Neurol* 332: 123–143

Ross HE, Young LJ (2009) Oxytocin and the neural mechanisms regulating social cognition and affiliative behavior. *Front Neuroendocrinol* 30: 534–547

Rupp AC, Ren M, Altimus CM, Fernandez DC, Richardson M, Turek F, Hattar S, Schmidt TM (2019) Distinct ipRGC subpopulations mediate light's acute and circadian effects on body temperature and sleep. *Elife* 8: e44358

Sherathiya VN, Schaid MD, Seiler JL, Lopez GC, Lerner TN (2021) GuPPy, a Python toolbox for the analysis of fiber photometry data. *Sci Rep* 11: 24212

Sonoda T, Li JY, Hayes NW, Chan JC, Okabe Y, Belin S, Nawabi H, Schmidt TM (2020) A noncanonical inhibitory circuit dampens behavioral sensitivity to light. *Science* 368: 527–531

Tam SKE, Hasan S, Hughes S, Hankins MW, Foster RG, Bannerman DM, Peirson SN (2016) Modulation of recognition memory performance by light requires both melanopsin and classical photoreceptors. *Proc R Soc B Biol Sci* 283: 20162275

Tang Y, Benusiglio D, Lefevre A, Hilfiger L, Althammer F, Bludau A, Hagiwara D, Baudon A, Darbon P, Schimmer J *et al* (2020) Social touch promotes interfemale communication via activation of parvocellular oxytocin neurons. *Nat Neurosci* 23: 1125–1137

Theodosis DT, Paut L, Tappaz ML (1986) Immunocytochemical analysis of the GABAergic innervation of oxytocin- and vasopressin-secreting neurons in the rat supraoptic nucleus. *Neuroscience* 19: 207–222

Valle FP (1970) Effects of strain, sex, and illumination on open-field behavior of rats. *Am J Psychol* 83: 103–111

Xiao L, Priest MF, Nasenbeny J, Lu T, Kozorovitskiy Y (2017) Biased oxytocinergic modulation of midbrain dopamine systems. *Neuron* 95: 368–384.e5

Yu H, Miao W, Ji E, Huang S, Jin S, Zhu X, Liu M-Z, Sun Y-G, Xu F, Yu X (2022) Social touch-like tactile stimulation activates a tachykinin 1-oxytocin pathway to promote social interactions. *Neuron* 110: 1051–1067.e7

Zhang Z, Beier C, Weil T, Hattar S (2021) The retinal ipRGC-preoptic circuit mediates the acute effect of light on sleep. *Nat Commun* 12: 5115